Immobilized AgZnO photocatalyst in Poly(acrylic acid) matrix synthesized in water suspension and their photocatalytic activity

A. B. Jasso-Salcedo[a], D. Meimaroglou[b], M. Camargo[b], S. Hoppe[b], F. Pla[b] and V. A. Escobar-Barrios[a]
[a]IPICYT, San Luis Potosí, S.L.P., Mexico, vladimir.escobar@ipicyt.edu.mx,
[b]CNRS-Université de Lorraine, Nancy, France, sandrine.hoppe@univ-lorraine.fr

ABSTRACT

Silver modified ZnO particles (1% wt. Ag/ZnO), using UV light, were immobilized on a 3D network of crosslinked poly(acrylic acid) through ester linkages using GLYMO as coupling agent. Water based free radical polymerization was used for synthesis of Ag/ZnO-poly(acrylic acid) composites with 5 to 11% wt. content of photocatalyst, homogeneously dispersed as verified by SEM analysis. The Ag/ZnO- poly(acrylic acid) composites showed a higher thermal stability compared with pure poly(acrylic acid).
The photocatalytic activity for bisphenol-A degradation was lower for the Ag/ZnO-poly(acrylic acid) composites (~50%) in comparison with the pure Ag/ZnO (>70%), but remained fairly constant after at least two consecutive reuse cycles.

Keywords: Ag/ZnO, Polymeric Composite, Photocatalysis, Bisphenol-A, Water Treatment.

1 BACKGROUND

Zinc oxide (ZnO) is a photocatalyst with an adequate efficiency for photodegradation of dyes and several organic molecules in aqueous solution [1,2]. However, this efficiency must be improved for photocatalysis under visible light. In this sense, the modification of ZnO with silver nanoparticles (AgNPs) reduces the photocorrosion [3], improves the absorption of visible light [4,5] and increases the photocatalytic activity [3-6] in comparison to pure ZnO. The role of AgNPs is to increase the half-life time of the primary (excited electrons and holes, e^{*}-h^{+}) and secondary active species (free radicals, i.e. $^{\bullet}OH$), thus inducing a positive effect on the photocatalytic behavior of ZnO.
In spite of a series of specific Ag/ZnO advantages (e.g., decreased charge-carriers recombination rate, photostabillity, low cost and non-toxicity), its application in pilot scale systems has not yet been exploited. This is mainly attributed to difficulties related to the photocatalyst recovery and the UV/visible light sorption efficiency.
Homogeneous dispersion and immobilization of the photocatalyst within a matrix may affect favorably the reactive sites availability, surface area for contact, quantum yield and diffusion processes. A recent application includes the immobilization of photocatalysts (e.g., TiO_2) into polymeric matrices for the degradation of dyes in aqueous solutions. Among the most commonly used polymeric matrices are polyaniline [7, 8], polystyrene [9], acrylates [10, 11] and polypyrrole [12]. In order for a matrix to be suitable for photocatalytic water treatment under UV/visible light irradiation, in batch or continuous reactors, it must be hydrophilic, transparent, photochemically stable and mechanically resistant. Acrylic polymers are hydrogels that allow effective water transport for contact with the target pollutants due to their hydrophilicity and high wettability (i.e., display a capacity to absorb large amounts of water with respect to their own weight). In addition, they are generally colorless and visually transparent which allows the penetration of light into the matrix.
Accordingly, in the present work, a silver modified ZnO photocatalyst is synthesized and immobilized in a poly(acrylic acid) (PAA) polymer matrix for the degradation of bisphenol-A in water.

2 EXPERIMENTAL

2.1 Ag/ZnO preparation

The functionalization procedure of ZnO (VP AdNano ZnO 20 DW, Degussa Co.) using 1% wt. of stabilized silver nanoparticles (CITD-Peñoles Mexico) and the coupling agent GLYMO (Dynasylan ®) is described in Figure 1.

2.2 Synthesis of Ag/ZnO-PAA composite

The Ag/ZnO-GLYMO photocatalyst was vigorously dispersed in de-ionized water using ultrasound (1 h) under vacuum to remove oxygen. The degased suspensions (5 to11% wt., 22.5 mL)

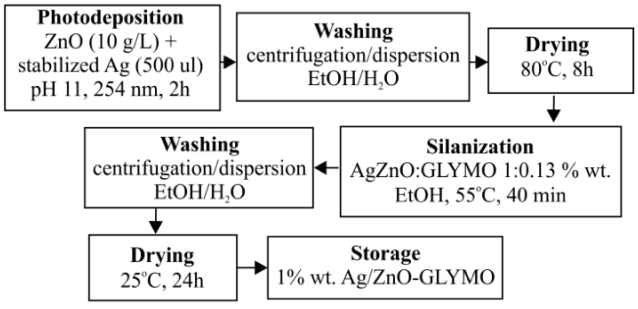

Figure 1. Flow diagram of the ZnO functionalization procedure.

and acrylic acid monomer (2.5 mL) were added to a triple-necked flask, stirred and heated in oil bath at 68°C under N_2 atmosphere. Potassium persulfate (KPS), sodium metabisulfite (SMBS) initiator and N, N-methylenebisacrylamide (MBA) crosslinker were added to the polymerization reactor and heated for 3 h. The residual components were removed by immersion of the final product composite into excess of water during 48 h.

2.3 Ag/ZnO and Ag/ZnO-PAA Composite characterization

The UV/Vis sorption was observed by solid-state UV-Vis spectroscopy (Varian Cary 4000 UV-Vis) from 300 to 600 nm wavelength. The morphology of pure Ag/ZnO photocatalyst was analyzed using a FEI TECNAI F30 STWIN G2 TEM microscope, while composites were observed using an ESEM FEI QUANTA 200 microscope. Fourier transform infrared spectrometry (FTIR-ATR ALPHA-P, Bruker) was used for the chemical analysis of Ag/ZnO, PAA and composites. The thermal stability of the synthesized photocatalyst was evaluated using a thermogravimetric analyzer (TGA/DCS 1, Mettler Toledo), under N_2 atmosphere and a heating rate of 30 °C/min from 200 °C to 700°C.

2.4 Photocatalytic Test

An aqueous solution of Bisphenol-A (80 mL, 10 ppm) and the photocatalyst were placed in a glass flask (i.e. photo-reactor), magnetically stirred and irradiated with UV (two lamps of 365 nm, 0.03 W/cm^2). The temperature was kept constant at 50°C. The pH of the solution was monitored during the photocatalytic tests (HAch sensION+ pH31 GLP pHmeter). After a defined UV irradiation time, aliquots of the solution were filtered (0.45 µm filter) and the concentration of Bisphenol-A was subsequently measured by liquid chromatography (UFLC, Shimadzu).

3 RESULTS AND DISCUSSION

3.1 Composite characterization

The interaction with light defines a large part of the photocatalytic behavior, for this reason the absorption of light needs to be considered. Figure 2A shows the UV-Vis spectra of the samples with two peaks: 360 and 437 nm. The first peak at 360 nm corresponds to ZnO absorbance due to the optical transition of electrons from valence band to conduction band in the semiconductor. The band gap (Eg) values, as estimated for the ZnO photocatalyst before and after the addition of silver, were equal to 3.20 eV and 3.24 eV, respectively. The second peak, at 437 nm, corresponds to the surface plasmon (SP) resonance of Ag nanoparticles. The shift of the broader SP peaks towards the visible region of the spectrum of Ag/ZnO, compared with the pure stabilized AgNPs, could be due to the strong interaction between Ag and ZnO as shown by the TEM images. Figure 2B shows the low magnified high-resolution

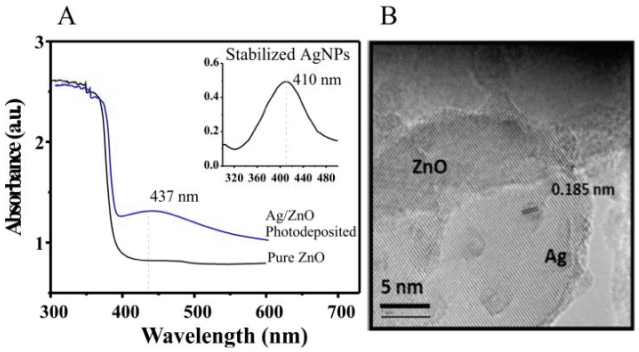

Figure 2. UV-Vis spectra (A) and TEM images (B) and of Ag/ZnO photocatalyst. Insert of (A) refers to the spectra of pure silver nanoparticles.

TEM images of Ag/ZnO with homogeneous distribution of Ag nanoparticles. The well-defined lattice fringes and continuity confirms the strong interaction between AgNPs and ZnO surface. Silver modification improves the spectral selectivity in the visible region and thus the overall photocatalytic behavior [13].

Surface modification of the nanoparticles has also been studied recently in order to synthesize polymeric composites with a broad range of applications [14]. Regarding this, coupling agents have been used to guarantee both the dispersion of nanoparticles and the linkage between modified nanoparticles and polymer. The advantage of GLYMO as coupling agent is the formation of self-assembled monolayers of silane with metal oxide surfaces, while the hydrocarbon tail creates a link with the polymeric matrix.

In the present study, the FTIR spectrum of Ag/ZnO shows disappearance of peaks at 823 and 780 cm^{-1}, corresponding to C-H from the metoxysilyl groups ($CH3O^-$) of GLYMO (data not shown), which indicates a methoxy group linkage to the ZnO surface through hydrogen bonds. In addition, the peak at 1030 cm^{-1}, corresponding to the formation of Si-O-Si layer on Ag/ZnO surface, confirms the silanization induced to prevent aggregation of the photocatalyst by

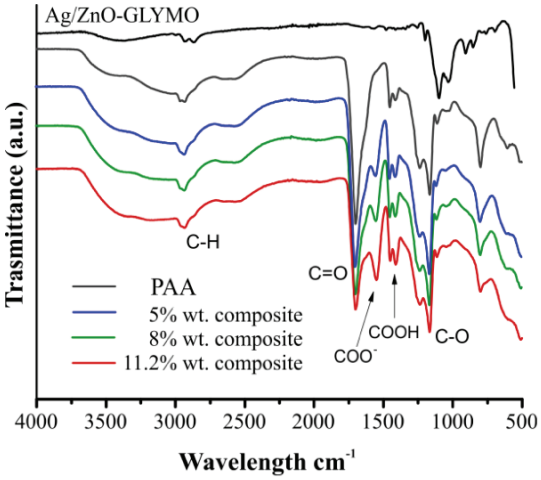

Figure 3. FTIR spectra of Ag/ZnO-PAA composites.

means of steric hindrance. On the other hand, the peaks at 1400, 1700 and 2940 cm^{-1} correspond to the characteristic carboxyl, carbonyl and -CH_2 groups of pure PAA, respectively (Figure 3). Regarding the Ag/ZnO-PAA composites, the FTIR spectra show similar peaks with the pure PAA. In addition, a new intense peak at 1540 cm^{-1} was assigned to the ionized carboxylate group (COO^-).

The SEM images of water-swollen samples (see Figure 4) clearly show the 3D structure of crosslinked PAA and the good dispersion of Ag/ZnO-GLYMO photocatalyst in the composites.

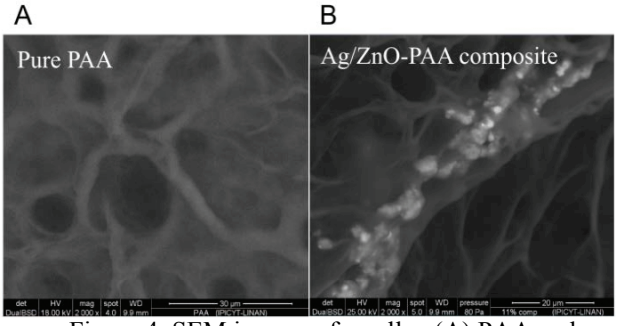

Figure 4. SEM images of swollen (A) PAA and (B) 11.2%wt. Ag/ZnO-PAA composite.

The ZnO particles appear to be embedded in the polymer chain forming a bead like line. The porous structure of both PAA and Ag/ZnO-PAA composites allows the water transport into the network of the hydrogel and interaction with the photocatalyst. To our knowledge, this is the first time that SEM evidence of the anchoring of Ag/ZnO particles on humid composites within the 3D crosslinked structure of PAA is provided.

Thermogravimetric analysis shows that the thermal stability of the PAA matrix displays a net increase with the Ag/ZnO nanoparticles content (Table 1, Column 4). Wu et al. [15] reported that among several composites of PAA-metal oxides (ZnO, CaO, CuO, etc.), the PAA-ZnO composite was the most thermally stable. Similar results are reported by Lu et al. [16].

Finally, the calculated amount of photocatalyst inside the polymeric matrix, obtained by subtraction of the PAA and Ag/ZnO-GLYMO residues from the corresponding Ag/ZnO-PAA composite residue, is in agreement with the nominal amount of photocatalyst added (see Table 1). This agreement of the nominal and calculated amount proves the homogeneous dispersion of Ag/ZnO photocatalyst inside the matrix.

Table 1. Thermogravimetric analysis data of PAA and Ag/ZnO-PAA composites.

Sample	Residue %	Calculated content % wt.	T_{50} (°C)[1]
Ag/ZnO-GLYMO	6.14	-	-
PAA	1.46	-	391.5
Ag/ZnO-PAA:			
5% wt. composite	12.71	5.11	420
8% wt. composite	20.19	8.28	443.5
11.2% wt. composite	20.15	10.41	447

[1] Temperature of 50% weight loss.

3.2 Photocatalysis test

Only a small fraction of bisphenol-A, equal to 8.2%, was destroyed by photolysis (i.e. UV light only), while this fraction increased to 18% when pure PAA was used (see Figure 5A). At the same time, in the presence of a Ag/ZnO-PAA composite, the photocatalytic degradation rate of bisphenol-A significantly increased, leading to an overall elimination of 47% of the pollutant (i.e., for the 8% wt. composite). Although this percentage is inferior to the result corresponding to the use of pure Ag/ZnO (i.e., 70%), it becomes evident that the immobilization of the photocatalyst can achieve comparable photodegradation efficiencies while providing a series of additional advantage

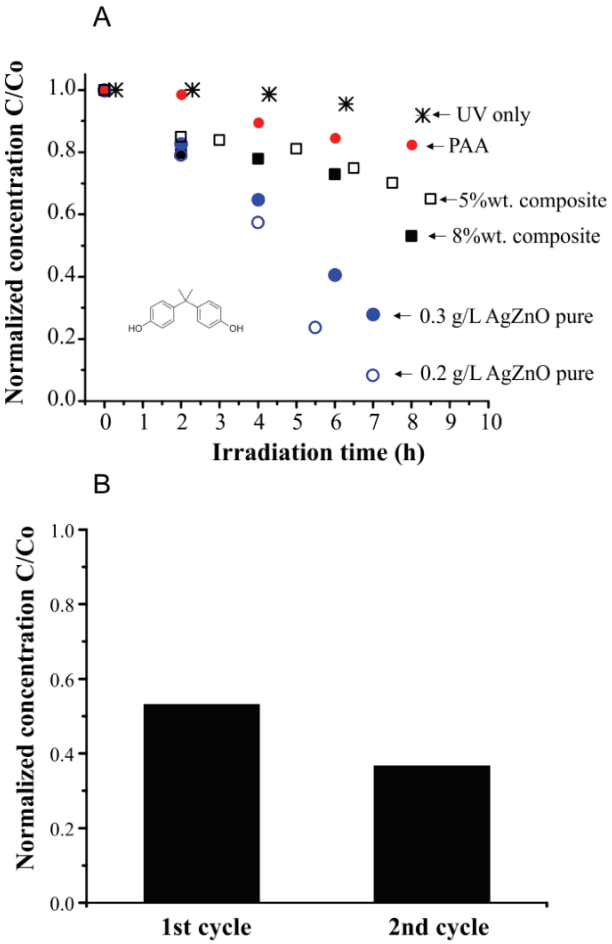

Figure 5. Photocatalytic performance in the degradation of bisphenol-A under UV light. (A) Comparison of the performance of the different photocatalysts with respect to radiation time, (B) overall photodegradation performance after one or two cycles of 8 h.

at the same time (e.g., reduced photocatalyst loses, possibility to implement continuous systems, etc.).

In an attempt to study the deterioration of the photocatalytic efficiency of the new photocatalyst, the 8% wt. Ag/ZnO-PAA composite was used in a second consecutive cycle without washing. The results show that its photocatalytic activity was kept relatively constant, corresponding to a photodegradation of bisphenol-A equal to 47% and 64%, for the 1st and 2nd cycles, respectively, as shown in Figure 5B.

Moreover, since no change in the chemical structure was detected by FTIR analysis (see Figure 6), it can be assumed that the poly(acrylic acid) matrix prevents the Ag/ZnO photocorrosion and conserves the photocatalytic sites for the next bisphenol-A degradation.

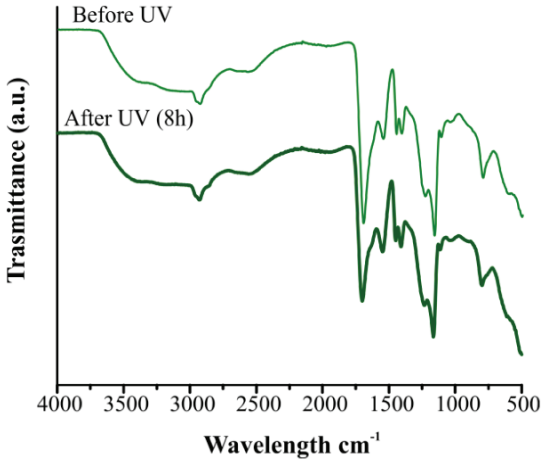

Figure 6. FTIR spectra of 8%wt. Ag/ZnO-PAA composite before and after 8 h of UV irradiation.

4 CONCLUSIONS

In this work, it was demonstrated that it is possible to synthesize photo and thermally stable Ag/ZnO-PAA composites, with homogeneously dispersed and chemically anchored Ag/ZnO photocatalyst particles (5-11.2% wt. content) in a poly(acrylic acid) matrix, by a surface modification with epoxide functional groups.

It was shown that the homogeneous distribution of silver modified ZnO within the matrix enhances the photocatalytic activity for bisphenol-A degradation. The photocatalytic sites in the composites remained active and lead to an efficient bisphenol-A degradation, as expected. Furthermore, the poly(acrylic acid) matrix prevented the photocorrosion of Ag/ZnO, making possible to reuse the composite in successive photodegradation cycles.

The proposed heterogeneous photocatalyst composites will be tested further for the degradation of emergent organic contaminants in water.

Acknowledgments. *The authors would like to thank the National Science and Technology Council of Mexico for the grant to ABJS (CONACYT-211830) and PCP project scholarchip (PCP-004-12). To Nicolás Cayetano, Ana Iris Peña Maldonado for technical support in TEM/SEM characterization at LINAN-IPICYT. To Emilien Girot and Steve Poinve for technical support in ENSIC-Lorraine Univesity.*

REFERENCES

[1] Sankthivel, S.; Neppolian, B.; Shankar, M.; Arabindoo, B.; Palanichamy, M.; Murugesan, V. Solar Energy Materials and Solar Cells 77, 65-82, 2003

[2] Zhang, L.; Yin, L.; Wang, C.; Lun, N.; Qi, Y. Applied Materials and Interfaces 2, 1769-1773, 2010.

[3] Xie, W.; Li, L.; Sun, W.; Huang, J.; Xie, H.; Zhao, X. Journal of Photochemistry & Photobiology, A: Chemistry 216, 149-155, 2010.

[4] Wang, X.M. Fan, K. Tian, Z.W. Zhou, Y. Wang, Applied surface Science 17, 7763-7770, 2011.

[5] F. Peng, H. Zhu, H. Wang, H, Yu Korean Journal of Chemical Engineering 24,1022-1026, 2008.

[6]Gouvêa, C.A.K.; Wypych, F.; Moraes, S.G.; Durán, N.; Peralta-Zamora, P. Chemosphere 40, 427-432, 2000.

[7] Leng, C.; Wei, J.; Liu, Z.; Xiong, R.; Pan, C.; Shi, J. J Nanopart Res 15, 164, 2013.

[8] Li, Y.; Yu, Y.; Wu, L. et al. Applied Surface Science 273, 135-143, 2013.

[9] Hecht, L.; Winkelmann, m.; Wanger, C.; Landfester, K.; Gerlinger, W.; Sachweh, B. Chem Eng Technol 9, 1670-1676, 2012.

[10] Wang, S.; Liu, Q.; Zhu, A. European Polymer Journal 47, 1168-1175, 2011.

[11] Kangwansupamonkon, W.; Jitbunpot, W.; Kiatkamjornwong, S. Polymer Degradation and Stability 95, 1894-1902, 2010.

[12] Lu, B.; Liu, M.; Shi, H.; Huang, X.; Zhao, G. Electroanalysis 25, 771-779, 2013.

[13] Jasso-Salcedo, A.B.; Palestino, G.; Escobar-Barrios, V.A. Journal of Catalysis *submitted*.

[14] Abdolmaleki, A.; Mallakpour, S.; Borandeh, S. Applied Surface Science 257, 6725-6733, 2011.

[15] Wu, H.; Jone, H.; Meng, S. Journal of Applied Polymer Science 66, 2021-2027, 1997.

[16] Yun, J.; Im, J.; Oh, A.; Jin, D.; Bae, T.; Lee, Y.; Kim, H. Materials Science and Engineering: B 176, 276-281, 2011.